Transactions of the Korean Nuclear Society Spring Meeting
Jeju, Korea, May 12-13, 2016

Effects of Misalignments on Microtomography

Jae Hong Hwang [a], Jong Hee Yun[a], Ho Kyung Kim [a, b*]
[a]*School of Mechanical Engineering, Pusan National University, Busan, South Korea*
[b]*Center for Advanced Medical Engineering Research, Pusan National University, Busan, South Korea*
[*]*Corresponding author: hokyung@pusan.ac.kr*

1. Introduction

Geometric misalignment is largely responsible for image quality of reconstructed images obtained from a micro-CT system, which typically has a spatial resolving power less than 0.1 mm. The geometric misalignment can include the translations of detector center position parallel to the y and z axes (i.e., Δu and Δv in the detector plane; refer to Fig. 1) with respect to the central beam and the detector rotations along *x*, *y*, and *z* axes (i.e, skewed η, tilted θ, and twisted ϕ, respectively; see Fig. 2). To avoid any distortions and/or artifacts that originate from the geometrical misalignments in reconstructed images, it is crucial to quantify those misalignments and then to reflect them into the image reconstruction procedure. It is typically known that the effect of η is the greatest in image quality of cone-beam CT [1,2].

Many studies have been carried out for quantitative measurements of misalignments. F. Noo *et al.* [3] proposed an analytic method based on ellipse parameters, which were extracted from projections for a two-ball phantom. This method cannot identify the tilted angle of a detector because it assumes that $\theta = 0$. A similar approach was introduced by K. Yang *et al.* [2], but it assumed that $\theta = \phi = 0$. On the other hand, D. Panetta *et al.* [4] introduced an optimization method, which did not require any phantoms, instead, used the object itself to be imaged for calibration. The sinogram, which should include features that could designate misalignments, was used as a cost function for the iterative optimization procedure. This approach may be attractive because it does not require any additional phantoms. However, it cannot determine all the misalignments as described above.

In this study, we investigate the effects of geometrical misalignments on the image quality of micro-CT. To determine the quantitative misalignments of our micro-CT system, we applied the ellipse-parameter method proposed by F. Noo *et al.* [3]. The micro-CT images obtained for a wire phantom and *ex-vivo* rabbit bone without and with geometrical calibration are compared in this study.

2. Materials and Methods

2.1 Laboratory Micro-CT System

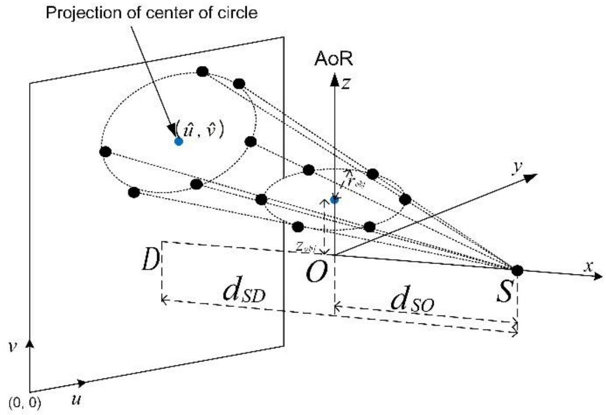

Figure 1. Schematic view describing the ball-phantom trajectory obtained at six projection angles in cone-beam CT geometry. The AoR coincides with the z axis. The distance from the source to the AoR and the detector are denoted by d_{SO} and d_{SD}, respectively. The shortest distance from the source to the detector plane is denoted by D. The distance from the AoR to the center of the ball is denoted by r_{obj} and the distance from the center of the circle to origin is denoted by z_{obj}. The symbols $\hat{u}$ and $\hat{v}$ denote the coordinates of the projected center of the circle.

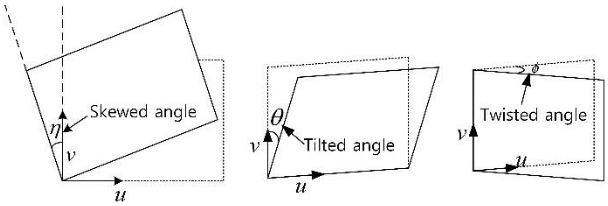

Figure 2. Rotational misalignments of the detector along main axes. The skewing, tilting, and twisting rotations are denoted by η, ϕ, and θ, respectively.

A micro-CT system with a flat-panel detector (FPD) was realized on an optical bench. During continuous x-ray irradiation, the object rotates on its axis by an amount of prescribed step angle and then the rotation stays until the FPD produces a projection image. Those motion and image readout were computer-controlled and lasted till the circular scan with a prescribed angular range completed. The distances from the x-ray focal spot to the FPD (d_{SD}) and from the focal spot to the axis of rotation (d_{SO}) were computer-controlled variables.

The FPD (Shad-o-Box 1548 HS, Teledyne Rad-icon Imaging Corp., Sunnyvale, CA) used a Gd_2O_2S:Tb-based phosphor (~68 mg cm^{-2}) for x-ray detection, and the optical photons from the phosphor were detected by a photodiode array made by complementary metal-oxide-semiconductor (CMOS) process. The CMOS photodiode had 0.099-mm sized pixels arranged in a

1548 × 1032 format. The maximum frame rate for reading out x-ray images was 20 frames per second (fps).

The x-ray source (Series 5000 XTF5011, Oxford Instruments, Inc.,U.S.A.) employed a tungsten anode and could operate up to the maximum power of 50 Watts. A 2-mm thick aluminum sheet was placed close at the beam exit of x-ray tube as an added filter. According to the manufacturer, the nominal focal-spot size was 0.035 mm.

For image reconstruction, the Feldkamp's CBCT algorithm [5] with the ramp filter was employed.

2.2 Calibration of Geometrical Misalignments

As shown in Fig. 1, the ball trajectories are determined from the projections for a two-ball phantom (in this example, only an upper ball-phantom trajectory obtained at six projection angles is shown for brevity). Then, we can obtain ellipse equations describing the ball trajectories by using the least-squares regression analysis. Applying the extracted two-ellipse parameter sets into the analytical algorithm [3], we determined that $\Delta u =$ 2.3 mm, $\Delta v = 0.5249$ mm, $\eta = 0.5585°$, $\phi = 0.05°$, $\Delta d_{SD} = 1.97$ mm, and $\Delta d_{SO} = 3.87$ mm.

2.3 Imaging

To investigate the effect of measured misalignments on the reconstructed images, we obtained images for a wire phantom and *ex-vivo* rabbit bone, as shown in Figs. 3 and 4, respectively. The imaging conditions were 45 kVp and 0.9 mA. The tomographic images for the two phantoms were obtained without and with geometrical calibration.

3. Results

Figure 5 compares the wire phantom images without and with geometrical calibration. Misalignments made the single-wire phantom appear in two wires, due to the relatively large Δu (note that the wire diameter was only 0.025 mm), as shown in Fig. 5(a), whereas the calibration successfully remedied this distortion artifact, as shown in Fig. 5(b).

Comparisons with rabbit bone are shown in Fig. 6, and the calibration dramatically enhances the tomographic image quality.

4. Further Study

We have investigated the effects of geometrical misalignments on micro-CT images. However, the study is limited to a qualitative investigation. For more detailed investigation, a phantom that can report quantitatively as a function of the extent of misalignments is being designed. The evaluation results of the geometrical misalignments on micro-CT image quality using the phantom will be reported.

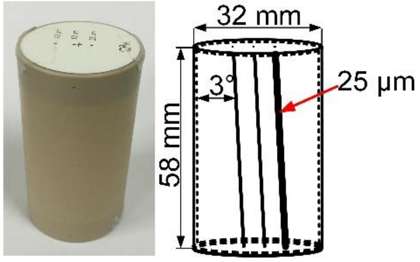

Figure 3. The wire phantom used for imaging.

Figure 4. The *ex-vivo* rabbit bone phantom used for imaging.

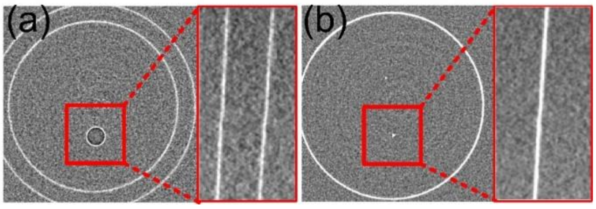

Figure 5. The tomographic images obtained for the wire phantom (a) without and (b) with the geometrical calibration.

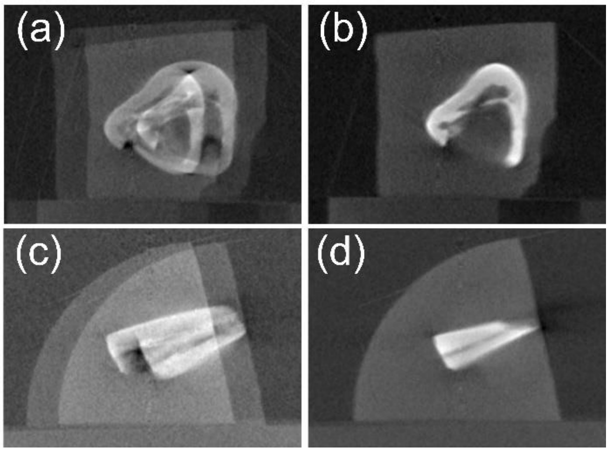

Figure 6. The tomographic images obtained for The *ex-vivo* rabbit bone phantom: (a) and (c) are obtained without calibration, and (b) and (d) with calibration.

ACKNOWLEDGMENTS

This work was supported by the National Research Foundation of Korea (NRF) grant funded by the Korea government (MSIP) (No. 2013M2A2A9046313).

REFERENCES

[1] C. Youngbin, J. M. Douglas, H. S. Jeffrey, and A. J. David, "Accurate technique for complete geometric calibration of cone-beam computed tomography systems," *Med. Phys.* **32** (2005) 968-983

[2] K. Yang, A. L. C. Kwan, D. F. Miller, and J. M. Boone, "A geometrical calibration method for cone beam CT systems," *Med. Phys.* **33** (2006) 1695-1706

[3] F. Noo, R. Clackdoyle, C. Menessier, T. A. White, and T. J. Roney, "Analytic method based on identification of ellipse parameters for scanner calibration in cone-beam tomography," *Phy. Med. Biol.* **45** (2000) 3489-3508

[4] D. Panetta, N. Belcari, A. Del. Guerra, and S. Moehrs, "An optimization-based method for geometrical calibration in cone-beam CT without dedicated phantoms," *Phy. Med. Biol.* **53** (2008) 3841-3861

[5] L. A. Feldkamp, L. C. Davis, and J. W. Kress, "Practical cone-beam algorithm," *J. Opt. Soc. Am. A* **6** (1984) 612-619